August, 1991] Bull. Chem. Soc. Jpn., 64, 2449—2453 (1991) 2449

X-Ray, Electrical and Catalytic Studies of the System $CoFe_2O_4$–Co_2TiO_4

Gulabshankar Ramkhelawan Dube and Vishnu Shivram Darshane*
Institute of Science, 15, Madam Cama Road, Bombay 400032, India
(Received October 18, 1990)

The system $Co_{1+x}Fe_{2-2x}Ti_xO_4$ has been studied with a view to investigating the cation distribution and to correlate the catalytic behavior of spinel with electrical and structural properties. To investigate cation distribution, techniques like X-ray diffraction, electrical conductivity, and thermo emf. have been used. The catalytic evaluation was carried out in the temperature range of 473—673 K using benzyl alcohol as a probe molecule. Our results show $CoFe_2O_4$ to be better catalyst for benzyl alcohol decomposition compared to Co_2TiO_4 or pure oxides of the system.

Oxidic spinels shows interesting electrical, magnetic, and catalytic properties. In these compounds, the properties are controlled by the nature of ions, their charge, and the site distribution amongst tetrahedral and octahedral sites. Several workers[1–3] have reported solid spinel solution of ferrites by substituting ions at tetrahedral and octahedral sites.

Ferrites have been used as efficient catalysts for the decomposition of alkenes,[4,5] hydrogen peroxide,[6,7] and alcohol.[8,9]

We have studied $CoFe_2O_4$–Co_2TiO_4 with a view to investigating the cation distribution and the effect of substitution on the tetrahedral and octahederal sites with reference to catalytic behavior.

Materials and Methods

The different compositions of the system were prepared by coprecipitation techniques.[10] A. R. grade soluble chlorides viz. $CoCl_2\cdot 6H_2O$, $TiCl_4$ (15% solution), and $FeCl_3\cdot 6H_2O$ were used to get Co^{2+}, Fe^{3+}, and Ti^{4+} ions in solution.

An aqueous solutions containing these ions in the required molar proportion were prepared by dissolving above salts in distilled water. The corresponding hydroxides were precipitated using 10% NaOH and maintaining the pH between 9.0 and 9.5. The precipitate was heated on water bath at 360 K for 3 h. and was then oxidized by adding calculated amount of 30% H_2O_2 (100% vol) with constant stirring. The precipitate was filtered, washed and dried in vacuum cryostat at 350 K for 2 h.

To measure electrical conductivity and thermoelectric power, pellets were prepared using 2% poly(vinyl acetate) solution as binder. The pellets were heated slowly in air (275 K min^{-1}.) to remove binder and then sintered at 1173 K.

The compositions of the product were checked by chemical analysis and were found to be in agreement with the theoretical values. The particle size was determined from XRD analysis and was found to be approximately 4 μm.

X-Ray powder patterns were recorded on diffractometer (Siemens D-Crystalloflex) using Cu *Kα* radiation with Ni-filter. X-Ray patterns of all the compositions indicated formation of single spinel phase. To measure the intensity, area under different *h k l* peaks were determined and the values obtained in relation to the peak area for 311 reflection was taken as 100. To calculate relative integrated intensity, *I*, of given *h k l* reflection, following formula[11] was used where notations have their usual meaning,

$$I_{hkl}=|F_{hkl}|^2\times P\times\frac{1+\cos^2 2\theta}{\sin^2\theta\cos\theta}$$

The atomic scattering power values for various ions were taken from International Table.[12] To determine cation distribution and it's variation with compositions, the intensity ratios I_{200}/I_{400}, I_{220}/I_{440},I_{422}/I_{400}, I_{400}/I_{422} for different possible models were calculated and compared with the observed intensity ratios.

DC resistivity measurements were carried out using LCR-Markoni bridge. The flat faces of each pellet were coated with thin layer of conducting silver paste and resistivity as well as thermo emf. measurements were carried out from room temperature to 673 K.

Each composition of the system has been investigated for its catalytic activity in the temperature range of 473—673 K. 3.0 g of the powdered catalyst was packed in a 25 cm long quartz

Table 1. Cation Distribution, Lattice Constant, Activation Energy (ΔE) and Thermoelectric Coefficient (α) of the System $Co_{1+x}Fe_{2-2x}Ti_xO_4$

Compositions (x)	Cation distribution		Lattice constant	Activation energy/eV	Thermo emf.coeff(α)
	A-site	B-site			
0.0	Fe^{3+}	$Co^{2+}Fe^{3+}_{1.0}$	8.368	0.52	−40.00
0.2	$Fe^{3+}_{0.8}Co^{2+}_{0.2}$	$Co^{2+}Fe^{3+}_{0.8}Ti^{4+}_{0.2}$	8.382	0.60	−10.00
0.4	$Fe^{3+}_{0.6}Co^{2+}_{0.4}$	$Co^{2+}Fe^{3+}_{0.6}Ti^{4+}_{0.4}$	8.395	0.68	+155.00
0.6	$Fe^{3+}_{0.4}Co^{2+}_{0.6}$	$Co^{2+}Fe^{3+}_{0.4}Ti^{4+}_{0.6}$	8.405	0.73	+198.00
0.8	$Fe^{3+}_{0.2}Co^{2+}_{0.8}$	$Co^{2+}Fe^{3+}_{0.2}Ti^{4+}_{0.8}$	8.410	0.79	+225.00
1.0	$Co^{2+}_{1.0}$	$Co^{2+}Ti^{4+}_{1.0}$	8.423	0.83	+255.00

Table 2. Comparison of Intensity Ratios for the Compound $Co_{1.6}Fe_{0.8}Ti_{0.6}O_4$

Cations at		I_{440}/I_{422}		I_{220}/I_{440}		I_{422}/I_{400}		I_{220}/I_{400}	
A-Site	B-Site	Obsd	Calcd	Obsd	Calcd	Obsd	Calcd	Obsd	Calcd
$Co^{2+}_{1.0}$	$Fe^{3+}_{0.8}Co^{2+}_{0.6}Ti^{4+}_{0.6}$		5.1		1.20		0.75		1.20
$Co^{2+}_{0.6}Fe^{3+}_{0.4}$	$Fe^{3+}_{0.4}Co^{2+}_{1.0}Ti^{4+}_{0.6}$	4.22	4.22	0.64	0.64	0.59	0.58	1.58	1.59
$Co^{2+}_{0.4}Ti^{4+}_{0.6}$	$Fe^{3+}_{0.8}Co^{2+}_{1.2}$		4.35		0.59		0.53		1.45
$Co^{2+}_{0.2}Fe^{3+}_{0.6}Ti^{4+}_{0.2}$	$Fe^{3+}_{0.2}Co^{2+}_{1.4}Ti^{4+}_{0.4}$		4.00		0.45		0.69		1.85

reactor with 10 mm internal diameter. The reactor was equipped with thermocouple to monitor the temperature of the catalyst bed. The vapours of benzyl alcohol were passed over catalyst and the products were condensed using conventional techniques and were analyzed by gas chromatography. The products were further confirmed by GCMS.

Results and Discussion

X-Ray diffractometer patterns of all the compositions showed single spinel phase. The results of X-ray analysis are given in Table 1. From table it is observed that all the compositions of the system possess cubic symmetry. The lattice constant increases linearly from $CoFe_2O_4$ to Co_2TiO_4 obeying Vegard's law. The increase in lattice constant from $CoFe_2O_4$ is due to replacement of Fe^{3+} by slight bigger Co^{2+} and Ti^{4+} ions at octahedral site.

The cation distribution between two sites in the system has been arrived at by X-ray intensity calculations. The observed and calculated intensity ratios for different models for the composition x=0.6 is given in Table 2. From table, it is observed that the model with Ti^{4+} at B-site, Co^{2+} both A- and B-sites while Fe^{3+} distributed equally between A- and B- site shows better agreement. Our results on cation distribution are in close agreement with the values reported earlier on $CoFe_2O_4$ and Co_2TiO_4.[13,14]

Electrical Properties: DC resistivity of the compounds of the system $Co_{1+x}Fe_{2-2x}Ti_xO_4$ measured as a function of temperature varied between 10^6 and 10^7 ohm-cm. The plot of $\log \rho$ vs. $10^3/T$ showed a linear nature obeying Wilsen's law.

$$\rho = \rho_0 \exp(\Delta E/KT).$$

High values of resistivity indicate that elements with stable oxidation state are present at B-site.

From Table 1, it is observed that with subsequent replacement of Fe^{3+} by Co^{2+} and Ti^{4+} activation energy increases. This is due to the fact that Ti^{4+} (d^0) orbitals have much lower energy i.e. they are very stable and are much more contracted than Fe^{3+} d-orbitals. Also as concentration of Fe^{3+} ion decreases in the lattice, the mobility of charge carriers decreases resulting in the increase in the activation energy.

Thermoelectric coefficient values of the series varied between −40.00 and +255.00 μV K^{-1}. The compounds with $x \leqslant 0.2$ are n-type while $0.4 \leqslant x \leqslant 1.0$ are p-type (Table 1) semiconductors. p-Type semiconductivity of cobalt rich compounds can be attributed to the formation fo Co^{2+}/Co^{3+} ion pairs but unfortunately the presence of Co^{3+} ions could not be detected from X-ray intensity calculations as the concentration may be very small.

Catalytic Studies: Decomposition of benzyl alcohol has been reported by several workers using pure metal

Table 3. Catalytic Performance Data for the Decomposition of Benzyl Alcohol

Catalyst bed temp/K	Conversion	% Selectivity	
	%	Benzaldehyde	Toluene
	Catalyst: $CoFe_2O_4$		
473	2.3	75.85	22.59
523	5.68	63.55	27.50
573	18.66	50.78	35.72
623	32.04	39.8	40.17
673	49.62	27.09	45.00
	Catalyst: $Co_{1.2}Fe_{1.6}Ti_{0.2}O_4$		
473	2.0	83.0	12.5
523	5.5	68.5	14.05
573	14.02	60.0	25.0
623	24.01	43.85	25.0
673	36.0	33.17	31.0
	Catalyst: $Co_{1.4}Fe_{1.2}Ti_{0.4}O_4$		
473	1.77	90.43	4.56
523	2.78	77.99	11.75
573	11.76	65.08	18.46
623	21.05	52.39	24.79
673	30.35	40.31	31.04
	Catalyst: $Co_{1.6}Fe_{0.8}Ti_{0.4}O_4$		
473	1.0	90.2	4.0
523	2.5	77.59	20.4
573	10.05	68.5	14.2
623	54.0	54.0	23.0
673	27.0	43.75	29.0
	Catalyst: $Co_{1.8}Fe_{0.4}Ti_{0.8}O_4$		
473	0.52	95.0	4.0
523	2.0	80.0	9.7
573	10.5	70.5	15.5
623	16.5	58.0	26.5
673	24.05	45.39	28.0
	Catalyst: $Co_2Ti_{1.0}O_4$		
473	0.442	97.62	2.26
523	1.83	85.47	7.52
573	8.0	72.73	13.86
623	14.0	60.99	20.83
673	22.45	47.02	26.43

oxides and various zeolites.[15–18] However literature survey indicates that not much work has been reported where spinels have been used as catalysts for the decomposition of benzyl alcohol.

Decomposition of benzyl alcohol mainly yields benzaldehyde and toluene.

$$C_6H_5CH_2OH \xrightarrow{\text{Catalyst}} C_6H_5CHO + 2H^*$$

$$C_6H_5CH_2OH + 2H^* \longrightarrow C_6H_5CH_3 + H_2O$$

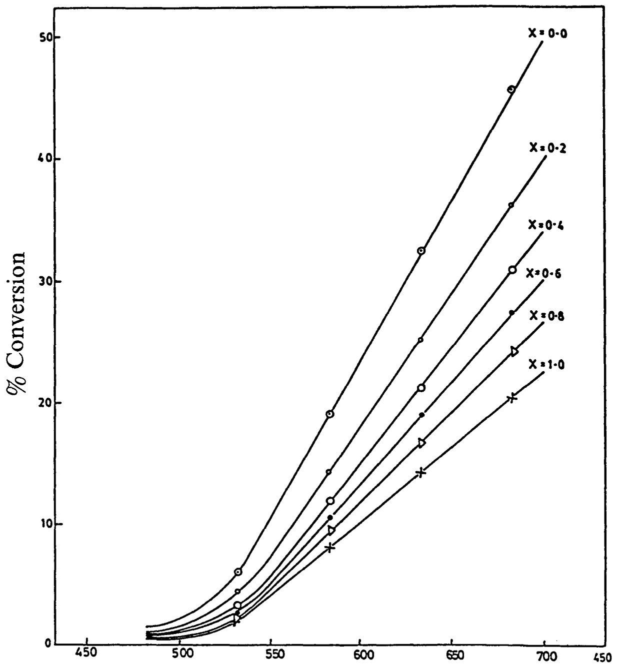

Fig. 1. Plot of % conversion of benzyl alcohol vs. temp over different compositions of the system $Co_{1+x}Fe_{2-2x}Ti_xO_4$.

Results of benzyl alcohol decomposition over various compositions of the system $Co_{1+x}Fe_{2-2x}Ti_xO_4$ are listed in Table 3. From table it is observed that conversion of benzyl alcohol on $CoFe_2O_4$ is always greater at all the temperatures compared to other catalyst compositions. The conversion of benzyl alcohol vs. temperature for the various compositions of the system is reported in Fig. 1. Further from Fig. 1 it is observed that conversion of benzyl alcohol decreases from $CoFe_2O_4$ to Co_2TiO_4. The decreases in the catalytic activity from cobalt-ferrite to cobalt titanate can be explained on the basis of cation distribution in the spinel.

$CoFe_2O_4$ being an inverse spinel, Fe^{3+} ions are present both, tetrahedral as well as octahedral site. Since Fe^{3+} can hop between +2 and +3 states, provide more active centers for the catalytic reaction. Therefore $CoFe_2O_4$ is more active. Subsequent replacement of Fe^{3+} by Co^{2+} and Ti^{4+} ions, an equivalent amount of Fe^{3+} ion is replaced by Co^{2+} at A-site while at B-site, it is substituted by Ti^{4+} ion. Thus B-site of the spinel system is occupied by the ions with stable oxidation state (Ti^{4+} and Co^{2+}) with increase in concentration of X which favors the formation of benzaldehyde, a dehydrogenation product.

With decrease in the iron(III) concentration in the spinel, toluene selectivity decreases and aldehyde selectivity increases indicating that ions at tetrahedral site are

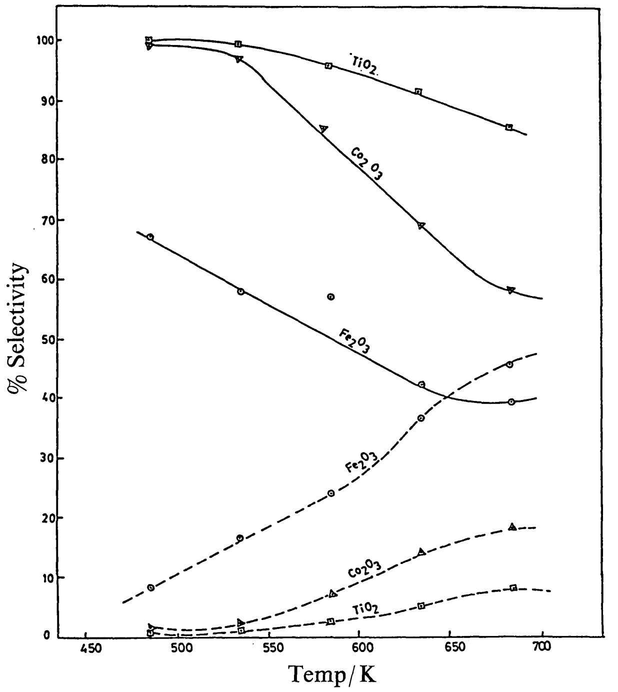

Fig. 2. Plot of aldehyde (——) and toluene (——) selectivity of pure oxides vs. temp of the system $Co_{1+x}Fe_{2-2x}Ti_xO_4$.

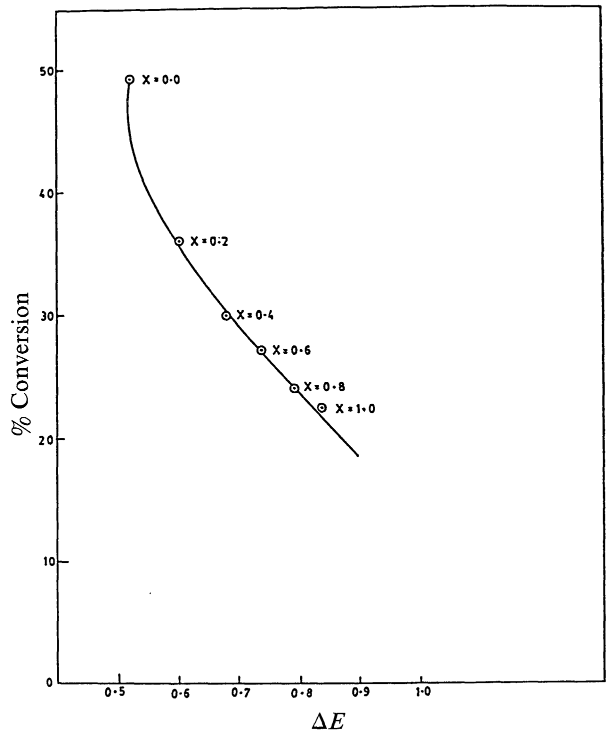

Fig. 3. Plot of % conversion vs. activation energy for the system $Co_{1+x}Fe_{2-2x}Ti_xO_4$ at 673 K.

responsible for the reduction of benzyl alcohol. Similar results have also been reported by Onchuku[19] in the investigation of decomposition of hydrogen peroxide using Cu–Ni–ferrite system.

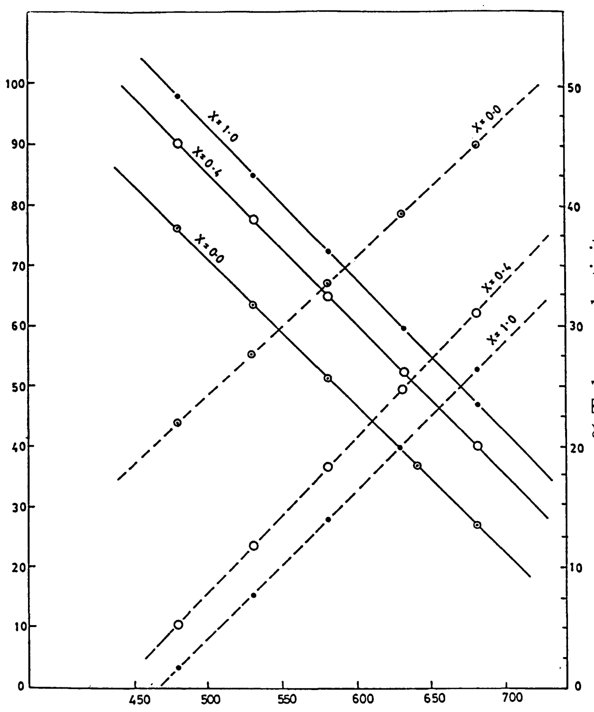

Fig. 4. Plot of % benzaldelyde and toluene selectivity over x=0.0, 0.4, and 1.0 for the system $Co_{1+x}Fe_{2-2x}Ti_xO_4$.

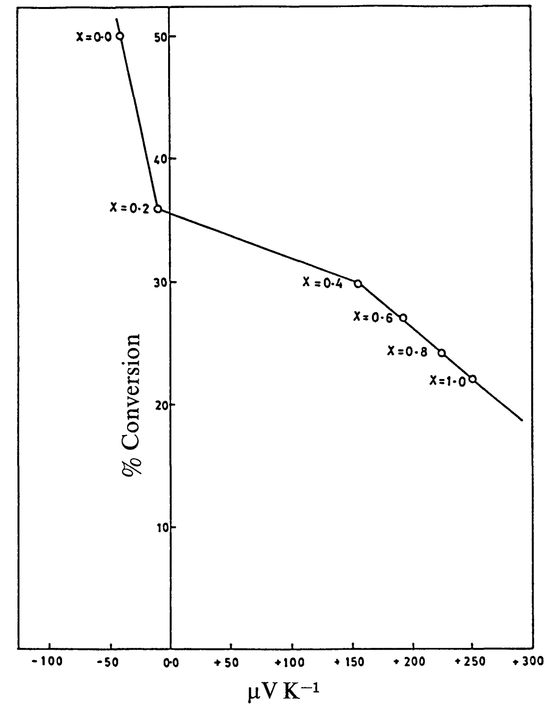

Fig. 5. Plot of % benzyl alcohol conversion vs charge carrier of the system $Co_{1+x}Fe_{2-2x}Ti_xO_4$.

The above observation is further supplemented by Fig. 2 which gives toluene selectivity over pure oxides of the system i.e. Fe_2O_3, Co_2O_3, and TiO_2. From Fig. 2 it is observed that Fe_2O_3 and Co_2O_3 yield maximum toluene while TiO_2 gives mainly benzaldehyde.

The substitution of Co^{2+} and Ti^{4+} results in the increase in the activation energy of the system from 0.52 eV ($CoFe_2O_4$) to 0.83 eV (Co_2TiO_4). Further from Fig. 3 it is noted that $CoFe_2O_4$ is the most active catalyst with the highest percentage conversion (49.62%) over any titanium containing compositions. The change in activation energy greatly influences the catalytic activity. The catalytic activity is due to transfer of electrons/holes from catalyst surface to substrate and is reversible. Hence greater the value of activation energy more will be the energy required for electronic transitions resulting in decrease in catalytic activity i.e. decrease in percentage benzyl alcohol decomposition.

From Fig. 4 it is observed that aldehyde selectivity increases and toluene selectivity decreases with increase in value of x. $CoFe_2O_4$ indicated 75.85% benzaldehyde selectivity at 473 K while at the same temperature Co_2TiO_4 showed 97.62% selectivity (Table 3).

It is well known that n-type semiconductors are always more active and selective towards dehydration of alcohols due to rapid migration of electrons while p-type semiconductors are active and selective towards dehydrogenation due to migration of holes.[20] The effect of nature of charge carriers on the catalytic activity of spinels is shown in Fig. 5. $CoFe_2O_4$ (α=40 µV K^{-1}) is most active for dehydration due to $Fe^{3+} \rightleftarrows Fe^{2+} + e^-$ hopping process (Table 3) where electrons are predominently the charge carriers. As the concentration of iron(III) decreases in the lattice ($x \geqslant 0.4$) the holes become predominent charge carriers result in decrease in overall catalytic activity.

Conclusion

Thus from X-ray intensity, electrical conductivity and thermo emf measurements the probable cation distribution of the system $Co_{1+x}Fe_{2-2x}Ti_xO_4$ is suggested as $Co_x^{2+}Fe_{1-x}^{3+}[Co_{1.0}^{2+}Fe_{1-x}^{3+}Ti_x^{4+}]\ O_4^{2-}$. Further it is observed that $CoFe_2O_4$ is most active catalyst towards benzyl alcohol decomposition while Co_2TiO_4 is most selective dehydrogenation catalyst.

References

1) Landolt-Borstein, "Magnetic Oxides and Related Compounds," Springer, Berlin (1970), Vol. 3/4b.

2) Prabha Nathwani and V. S. Darshane, *Pramana—J. Phys.*, **28**, 675 (1987).

3) A. Meenakshisundaram and V. Srinivasan, *Phys. Status Solidi A*, **69**, K15 (1973).

4) Renard, Jr. and W. H. Kehl, *J. Catal.*, **22**, 452 (1975).

5) W. Ronald Cares and Joe W. Hightower, *J. Catal.*, **39**, 36 (1975).

6) J. R. Goldstein and A. C. C. Tseung, *J. Catal.*, **32**, 452

(1974).

7) H. M. Cota, M. Chin, and F. J. Schoenweis, *Nature,* **19**, 1281 (1964).

8) P. K. Sharpe, J. C. Vickerman, and M. H. Stancy, Proce. 6th Internat. Cong. Catal., London (1976).

9) M. V. Joshi, V. G. Khanwalkar, and V. S. Darshane, "Advances in Ferrites," (1989), Vol. II, p. 1191.

10) P. M. Khopkar, J. A. Kulkarni, and V. S. Darshane, *Thermochim. Acta,* **93**, 481 (1985).

11) M. J. Burger, "Crystal Structure Analysis," John Wiley, New York (1960).

12) "International Tables for X-Ray Crystallography," Kynoch, Bermingham (1974), Vol. 4, pp. 72—98.

13) Prabha Nathwani and V. S. Darshane, *J. Phys. C, Solid State Phys.,* **21**, 3191 (1988).

14) J. K. Shrivastava, J. A. Kulkarni, S. Ramkrishnan, S. Singh, V. R. Marathe, G. Chandra, V. S. Darshane, and R. Vijayaraghavan. *J. Phys. C, Solid State Phys.,* **20**, 2139 (1987).

15) Ishinge Mayashosi, Sakal Koji, Kawai Mashutoshi, Hata Kajuo, *Bull. Chem. Soc. Jpn.,* **43**, 2186 (1970).

16) C. N. Pillai, M. Jayamani, and N. Murgesan, *J. Catal.,* **85**, 527 (1965).

17) S. Walter Trahanvoski and Brewster L. Young, *J. Chem. Soc.,* **8**, 5777 (1965).

18) Takatome and Kazushige, *Nagasaki Daigaku, Kyoikugakubu, Shizen Kagakukenkyu Hokoku,* **34**, 31 (1983).

19) A. I. Onchuku, *J. Chem. Soc., Faraday Trans. 1,* **80**, 1447 (1984).

20) O. V. Krylov, "Catalysis by Non-Metals," Academic Press, New York (1970).